

# Irreversible single-crystal to polycrystal and reversible single-crystal to single-crystal phase transformations in cyanurates

**MenaheM Kaftory,\* Mark Botoshansky, Moshe Kapon and Vitaly Shteiman**

Department of Chemistry, Technion–Israel Institute of Technology, Haifa 32000, Israel

Correspondence e-mail: kaftory@tx.technion.ac.il

Received 13 April 2001

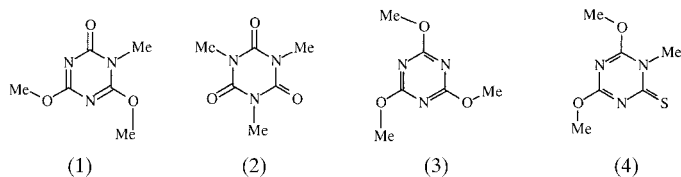
Accepted 26 September 2001

4,6-Dimethoxy-3-methyl-dihydrotriazine-2-one (1) undergoes a single-crystal to single-crystal reversible phase transformation at 319 K. The low-temperature phase crystallizes in monoclinic space group  $P2_1/n$  with two crystallographically independent molecules in the asymmetric unit. The high-temperature phase is obtained by heating a single crystal of the low-temperature phase. This phase is orthorhombic, space group  $Pnma$ , with the molecules occupying a crystallographic mirror plane. The enthalpy of the transformation is  $1.34 \text{ kJ mol}^{-1}$ . The small energy difference between the two phases and the minimal atomic movement facilitate the single-crystal to single-crystal reversible phase transformation with no destruction of the crystal lattice. On further heating, the high-temperature phase undergoes methyl rearrangement in the solid state. 2,4,6-Trimethoxy-1,3,5-triazine (3), on the other hand, undergoes an irreversible phase transformation from single-crystal to polycrystalline material at 340 K with an enthalpy of  $3.9 \text{ kJ mol}^{-1}$ ; upon further heating it melts and methyl rearrangement takes place.

## 1. Introduction

According to McCrone (1965), 'a polymorph is a solid crystalline phase of a given compound resulting from the possibility of at least two different arrangements of the molecules of that compound in the solid state'. This is a very general definition that states nothing about the way the polymorphs are being prepared or what the conditions are for their existence. In most cases different polymorphs are being prepared (or obtained with no intention) by varying crystallization conditions. The transformation of one polymorph to the other can be accomplished by heating (or cooling) if they are enantiotropic. Phase transitions in molecular solid compounds are of high importance in solid-state chemistry and in material science. Besides their importance, the mechanisms of transformations in molecular crystals are largely unknown (Dunitz & Bernstein, 1995). From energy considerations it is believed that the differences between polymorphs are usually quite small (Kitaigorodskii, 1970) and that they are temperature dependent. The dependence on temperature is due to the difference between the entropy of the polymorphs. If there are large differences between the structures of the polymorphs then usually the crystal lattice of the transformed phase is destroyed and followed by nucleation and growth of the new phase (Mnyukh, 1977, 1979). It is not clear to what extent may the structures of the two polymorphs be different and yet allowing transformation without destruction of the crystal

lattice. A certain level of understanding the mechanism of phase transitions is claimed for the order–disorder-type phase transformation. For this type of phase transformation there is only a slight difference between the site symmetries of the structural units of the two phases. The molecule of the higher-temperature phase adopts higher symmetry attributed to the time-averaged disordered molecules. There are examples of first-order phase transitions where the crystal lattice remains undestroyed during the transformation process. 1,2,4,5-Tetrabromobenzene has a first-order phase transformation at 319.5 K (Gafner, 1960, 1964). There is a very close resemblance between the crystal structures of the two polymorphs; both crystallize in the monoclinic space group  $P2_1/a$ . The enthalpy of transformation was measured as  $659 \text{ J mol}^{-1}$  (at 315 K; Herbstein, 2000). A second example is the single-crystal to single-crystal transformation of oxitropium bromide (Zamir *et al.*, 1994) that belongs to the class of thermosalient solids (jumping crystals). The two forms adopt an orthorhombic space group  $P2_12_12_1$ . There is a small difference between the molecular structures in the two forms and the enthalpy of the transition was measured to be  $2.5 \text{ kJ mol}^{-1}$ . During our study of methyl rearrangement in the solid state (Kaftory & Handelsman-Benory, 1994; Handelsman-Benory *et al.*, 2000; Greenberg *et al.*, 2001) we have found that there are two polymorphs of 4,6-dimethoxy-3-methyl-dihydro-triazine-2-one (1), 2,4,6-trimethoxy-1,3,5-triazine (3) and 4,6-dimethoxy-3-methyl-1,3,5-triazine-2(3*H*)-thione (4). The first crystallizes in only one form but undergoes phase transformation to the second polymorph. The last two compounds can be crystallized in two polymorphic forms and each of them also undergoes phase transformations. In the present publication we describe two different types of phase transitions observed in these compounds: irreversible single-crystal to polycrystal and reversible single-crystal to single-crystal.



## 2. Experimental

All compounds were prepared according to known procedures (Paolini & Tosato, 1968; Tosato, 1979, 1982).

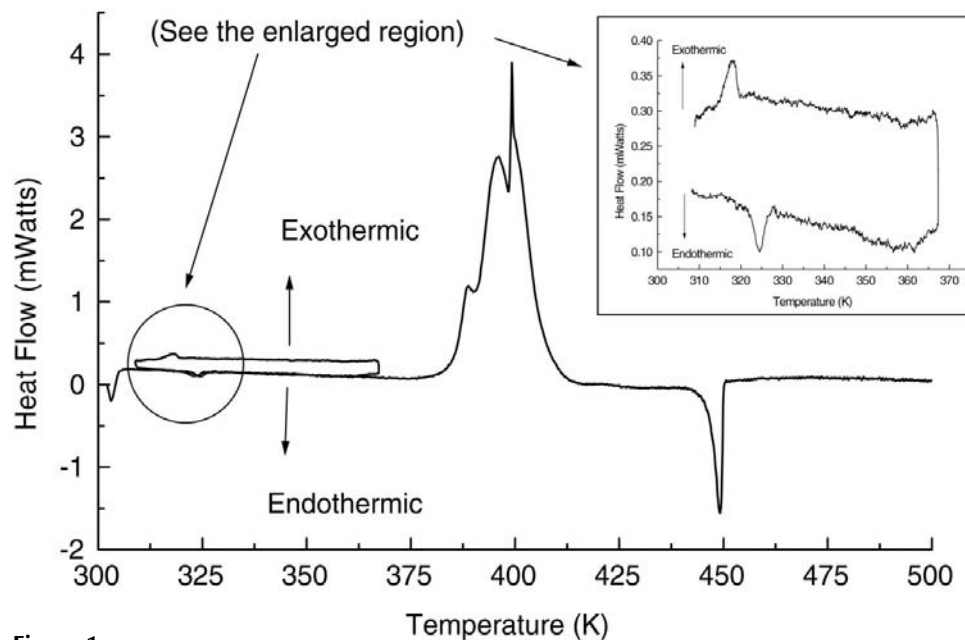


**Figure 1**  
DSC thermograph of (1) and (2) taken at a heating rate of  $1^\circ \text{ min}^{-1}$ , and enlargement of the encircled region.

The thermal behavior was studied using a Mettler DSC TA-3000 and Polymer Laboratory DSC-PL. NMR spectra were collected on Bruker AC200 and AC400 spectrometers.

The X-ray diffraction intensities at 359 K were measured using a Siemens SMART diffractometer. Crystallographic data are given as supplementary material.<sup>1</sup> Crystallographic data at 298 and 320 K are given in Table 1. Although the crystal structure of (1) at room temperature has been previously published (Handelsman-Benory *et al.*, 1995), we have repeated the X-ray diffraction intensity measurements and refined the crystal structures of the low- and high-temperature phases in the same way. All methyl H atoms have been calculated and refined as riding on their C atoms. One of the methyl H atoms at the high-temperature phase (C4) was found to be disordered between two conformations.

## 3. Results and discussion

The thermal behavior of the solid-state methyl rearrangement of 4,6-dimethoxy-3-methyl-dihydro-triazine-2-one (1) to 1,3,5-trimethyl-2,4,6-trioxohexahydro-*s*-triazine (2) was studied by measuring the enthalpy with a Differential Scanning Calorimeter (DSC; see the thermograph shown in Fig. 1). The exothermic peaks, starting at 380 K, were attributed to a solid-state intermolecular methyl transfer (Kaftory & Handelsman-Benory, 1994; Handelsman-Benory *et al.*, 2000); the endothermic peak at 448 K was assigned to the melting of the rearrangement product. The tiny peak (encircled in Fig. 1) was overlooked. The X-ray diffraction intensities were measured

<sup>1</sup>Supplementary data for this paper are available from the IUCr electronic archives (Reference: AV0042). Services for accessing these data are described at the back of the journal.

at elevated temperatures in an attempt to follow the variation of the atomic displacement parameters of the atoms involved in the rearrangement as a function of temperature. It was found that the crystal structures at temperatures above 319 K are different from those at lower temperature. It turned out that the low-temperature phase (LTP) crystallizes in the

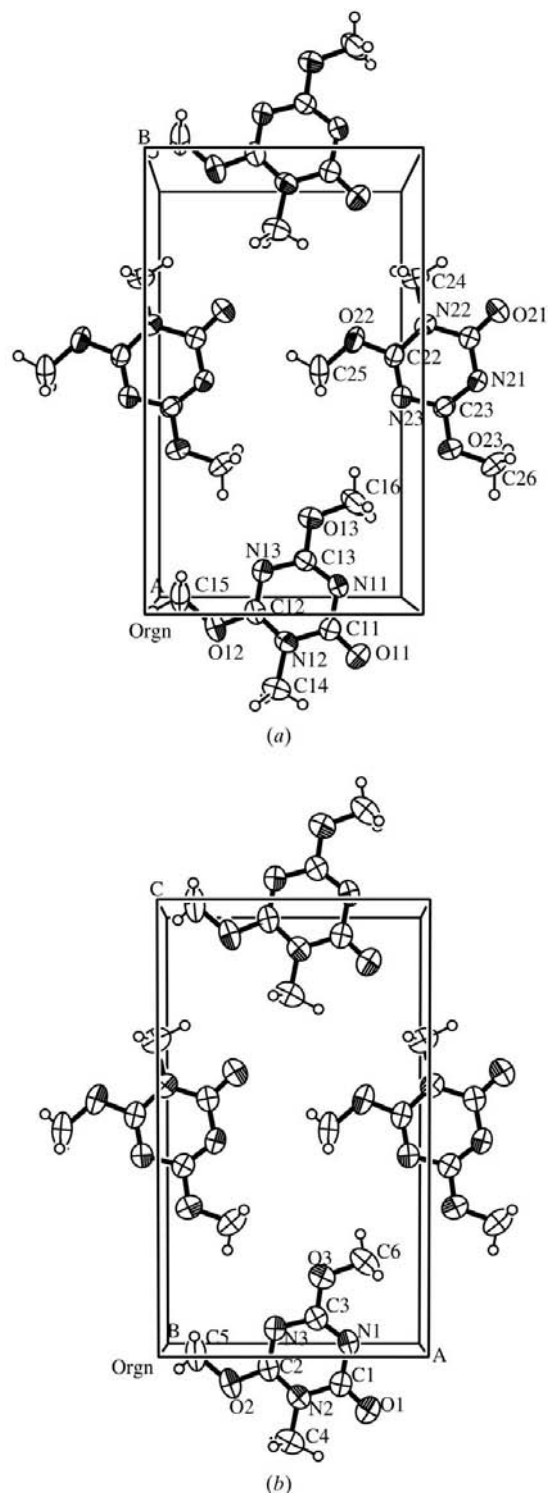


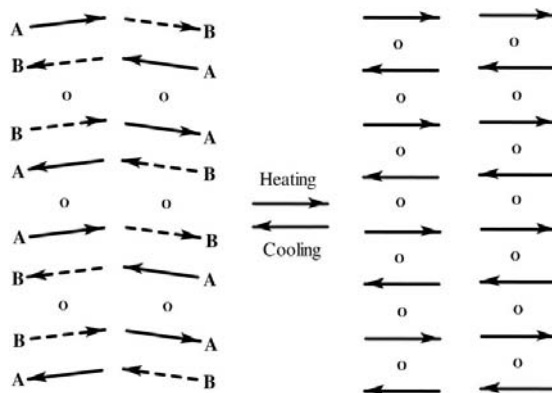
**Figure 2**  
A layer (a) of the low-temperature phase and (b) the high-temperature phase.

monoclinic space group  $P2_1/n$ , while crystals of the high-temperature phase (HTP) belong to the orthorhombic space group  $Pnma$ . Moreover, it was found that the high-temperature single crystal reverses to the low-temperature phase when the crystal was cooled to room temperature. It was therefore assumed that the overlooked peak represents a reversible phase transformation (see the enlarged encircled region in Fig. 1). There is ca  $3^\circ$  hysteresis between the phase transformation temperatures. The enthalpy ( $\Delta H$ ) of the phase transition is  $1.34 \text{ kJ mol}^{-1}$ , the entropy difference ( $\Delta S$ ) at 319 K is only  $4.2 \text{ J mol}^{-1} \text{ K}^{-1}$ .

### 3.1. Crystal structures of the LTP and HTP of (1)

The LTP crystallizes in the monoclinic space group  $P2_1/n$  with two crystallographically independent molecules in the asymmetric unit. The molecules are packed in columns parallel to the  $a$  axis and these form layers with molecules tilted in the  $bc$  plane (top view is shown in Fig. 2a and stereoscopic side view is shown in Fig. 3).

Neighboring columns are related by a glide plane and the angle between the molecular planes of these columns is  $15.77(3)^\circ$  (see Fig. 3, top). Each column consists of pairs of the two independent molecules  $A$  and  $B$ . The two molecules within a stack are parallel to each other and are arranged in the order  $A-B-B-A-A-B\dots$



While a crystallographic inversion center exists between the pairs, a pseudo-inversion center relates the two independent molecules. Irregular distances between the centers of the six-membered rings within a column of  $3.687(3)$  and  $3.442(3)$  Å exist between pairs of molecules related by the crystallographic inversion centers at  $A\cdot A$  and  $B\cdot B$ , respectively. The center-to-center distance between the two independent molecules is  $3.484(3)$  Å. The high-temperature phase is orthorhombic with space group  $Pnma$ . The molecules lie on crystallographic mirror planes. The molecules are packed in parallel columns similar to those of the low-temperature phase (see Figs. 2b and Fig. 3b). The distance between the centers of the rings related by an inversion center within a column is  $3.491(4)$  Å.

### 3.2. Comparison between the structural parameters

Crystallographic data for the two phases are given in Table 1. Fractional atomic coordinates for the LTP and HTP have

**Table 1**  
Experimental details.

	LTP	HTP
Crystal data		
Chemical formula	C <sub>6</sub> H <sub>9</sub> N <sub>3</sub> O <sub>3</sub>	C <sub>6</sub> H <sub>9</sub> N <sub>3</sub> O <sub>3</sub>
Chemical formula weight	171.16	171.16
Cell setting, space group	Monoclinic, <i>P</i> <sub>2</sub> <sub>1</sub> / <i>n</i>	Orthorhombic, <i>Pnma</i>
<i>a</i> , <i>b</i> , <i>c</i> (Å)	13.480 (2), 14.172 (2), 8.433 (1)	8.465 (1), 6.749 (1), 14.284 (2)
$\beta$ (°)	92.07 (2)	90
<i>V</i> (Å <sup>3</sup> )	1610.0 (2)	816.0 (2)
<i>Z</i>	8	4
<i>D</i> <sub>x</sub> (Mg m <sup>-3</sup> )	1.412	1.393
Radiation type	Mo <i>K</i> α	Mo <i>K</i> α
No. of reflections for cell parameters	3758	2809
$\theta$ range (°)	1.0–28.2	1.0–25.9
$\mu$ (mm <sup>-1</sup> )	0.115	0.113
Temperature (K)	298 (2)	320 (2)
Crystal form, color	Prism, colorless	Prism, colorless
Crystal size (mm)	0.35 × 0.3 × 0.3	0.35 × 0.3 × 0.3
Data collection		
Diffractometer	Nonius KappaCCD	Nonius KappaCCD
Data collection method	$\varphi$ scans	$\varphi$ scans
No. of measured, independent and observed parameters	3758, 3758, 2273	2809, 854, 487
Criterion for observed reflections	<i>I</i> > 2σ( <i>I</i> )	<i>I</i> > 2σ( <i>I</i> )
<i>R</i> <sub>int</sub>	0.046	0.0532
$\theta_{\max}$ (°)	28.26	25.89
Range of <i>h</i> , <i>k</i> , <i>l</i>	–17 → <i>h</i> → 17 –18 → <i>k</i> → 0 0 → <i>l</i> → 10	–10 → <i>h</i> → 10 0 → <i>k</i> → 8 –17 → <i>l</i> → 16
Refinement		
Refinement on	<i>F</i> <sup>2</sup>	<i>F</i> <sup>2</sup>
<i>R</i> [ <i>F</i> <sup>2</sup> > 2σ( <i>F</i> <sup>2</sup> )], <i>wR</i> ( <i>F</i> <sup>2</sup> ), <i>S</i>	0.0559, 0.1803, 1.041	0.0461, 0.147, 0.976
No. of reflections and parameters used in refinement	3758, 224	854, 102
H-atom treatment	Mixed	Mixed
Weighting scheme	$w = 1/[\sigma^2(F_o^2) + (0.0773P)^2 + 0.7666P]$ , where $P = (F_o^2 + 2F_c^2)/3$	$w = 1/[\sigma^2(F_o^2) + (0.0911P)^2 + 0.0000P]$ , where $P = (F_o^2 + 2F_c^2)/3$
( $\Delta/\sigma$ ) <sub>max</sub>	0.158	0.117
$\Delta\rho_{\max}$ , $\Delta\rho_{\min}$ (e Å <sup>-3</sup> )	0.223, –0.184	0.145, –0.161
Extinction method	<i>SHELXL</i>	<i>SHELXL</i>
Extinction coefficient	0.046 (7)	0.12 (3)

Computer programs used: *KappaCCD* (Nonius, 1998), *DENZO-SMN* (Otwinowski & Minor, 1997), *SHELXS97* (Sheldrick, 1997a), *SHELXL97* (Sheldrick, 1997b), *SMART*, *SAINT* (Siemens, 1995), *ORTEP3* (Farrugia, 1997).

**Table 2**  
Comparison between bond lengths (Å) of LTP and HTP of (1).

	LTP ( <i>A</i> )	LTP ( <i>B</i> )	320 K	359 K
O11–C11	1.221 (3)	1.220 (3)	1.212 (4)	1.212 (3)
O12–C12	1.321 (3)	1.319 (2)	1.317 (3)	1.320 (2)
O12–C15	1.458 (3)	1.457 (3)	1.456 (5)	1.460 (3)
O13–C13	1.330 (3)	1.333 (2)	1.338 (4)	1.328 (3)
O13–C16	1.445 (3)	1.447 (3)	1.454 (5)	1.449 (3)
N11–C13	1.297 (3)	1.297 (3)	1.295 (4)	1.289 (3)
N11–C11	1.369 (3)	1.367 (3)	1.362 (4)	1.354 (3)
N12–C12	1.348 (3)	1.349 (3)	1.346 (4)	1.341 (3)
N12–C11	1.402 (3)	1.406 (3)	1.393 (4)	1.403 (3)
N12–C14	1.469 (3)	1.469 (3)	1.480 (4)	1.478 (3)
N13–C12	1.304 (3)	1.306 (3)	1.303 (4)	1.297 (3)
N13–C13	1.350 (3)	1.350 (2)	1.342 (4)	1.357 (3)

been deposited. Crystallographic data, fractional atomic coordinates for the high-temperature phase at 359 K, coordinates of the H atoms, anisotropic displacement parameters

and tables of bond lengths corrected for libration are also given as supplementary material. Comparisons between bond lengths and angles of the two independent molecules of (1) at room temperature and a single molecule of the high-temperature phase at 320 and 359 K are given in Tables 2 and 3, respectively.

There are no significant differences between the intramolecular geometries at the three different temperatures. Comparison between the intermolecular distances (shorter than 4.0 Å, see Table 4) within a layer shows that the sum of the absolute values of the differences between intermolecular distances of the low- and the high-temperature phases is only 0.596 Å, indicating that there are no significant atomic displacements within the layers during the phase transformation. The differences between the intermolecular distances within the stacks, on the other hand, are important for the interpretation of the phase transformation. The overlap within each pair in a stack is shown in Fig. 4. The arrangement of molecules within a stack of LTP is such that there are two pairs (*A*·*A* and *B*·*B*) crystallographically related by inversion centers and a pair (*A*\**B*)

where the two molecules are related by a pseudo-inversion center. In the structure of the HTP there is only a single pair related by a crystallographic inversion center.

The overlap diagrams of the two pairs, *A*\**B* and *B*·*B*, in the LTP structure are similar to that of the single pair type in the HTP structure. The two molecules are shifted in opposite directions parallel to the N1–C3 bond (the atomic numbering is according to the HTP). The overlap diagram of one pair (*A*·*A*) in the LTP structure is significantly different and may be described in terms of a lateral shift of the two molecules in opposite directions parallel to the N11–C11 bond (see Fig. 4). The intermolecular distances between the six atoms of the ring in each pair are compared in Table 5 and in Fig. 5. Fig. 5 shows that the intermolecular distances of the two pairs *A*\**B* and *B*·*B* are very close to that in the HTP, while the intermolecular distances of the *A*·*A* pair are significantly different. It was found that the sum of the absolute values of differences

**Table 3**  
Comparison between bond angles ( $^{\circ}$ ) of LTP and HTP of (1).

	LTP (A)	LTP (B)	320 K	359 K
C12–O12–C15	116.9 (2)	116.8 (2)	117.0 (3)	116.8 (2)
C13–O13–C16	118.1 (2)	117.7 (2)	117.1 (3)	117.5 (2)
C13–N11–C11	116.8 (2)	117.1 (2)	116.7 (2)	117.4 (2)
C12–N12–C11	118.8 (2)	118.7 (2)	119.0 (3)	118.9 (2)
C12–N12–C14	122.2 (2)	122.3 (2)	122.7 (3)	122.5 (2)
C11–N12–C14	118.9 (2)	119.0 (2)	118.3 (3)	118.6 (2)
C12–N13–C13	113.6 (2)	113.5 (2)	113.4 (3)	113.4 (2)
O11–C11–N11	123.3 (2)	123.6 (2)	122.7 (3)	123.8 (2)
O11–C11–N12	119.0 (2)	118.8 (2)	119.5 (3)	118.7 (2)
N11–C11–N12	117.7 (2)	117.6 (2)	117.8 (3)	117.5 (2)
N13–C12–O12	121.5 (2)	121.7 (2)	122.0 (3)	121.5 (2)
N13–C12–N12	124.4 (2)	124.5 (2)	124.1 (3)	124.5 (2)
O12–C12–N12	114.1 (2)	113.8 (2)	113.9 (3)	114.0 (2)
N11–C13–O13	119.9 (2)	119.6 (2)	119.6 (3)	120.2 (2)
N11–C13–N13	128.7 (2)	128.7 (2)	129.0 (3)	128.3 (2)
O13–C13–N13	111.4 (2)	111.8 (2)	111.4 (3)	111.4 (2)

between the intermolecular distances in each pair in the LTP and in the HTP are 2.862, 0.559 and 0.612 Å for pairs *A*–*A*, *A*\**B* and *B*–*B*, respectively. A conclusion may be derived that most of the geometric adjustment during the phase transformation involves the *A*–*A* pair.

### 3.3. The phase transitions

Aromatic and other planar rings are usually packed in either stacks or herringbone motifs. Therefore, polymorphism

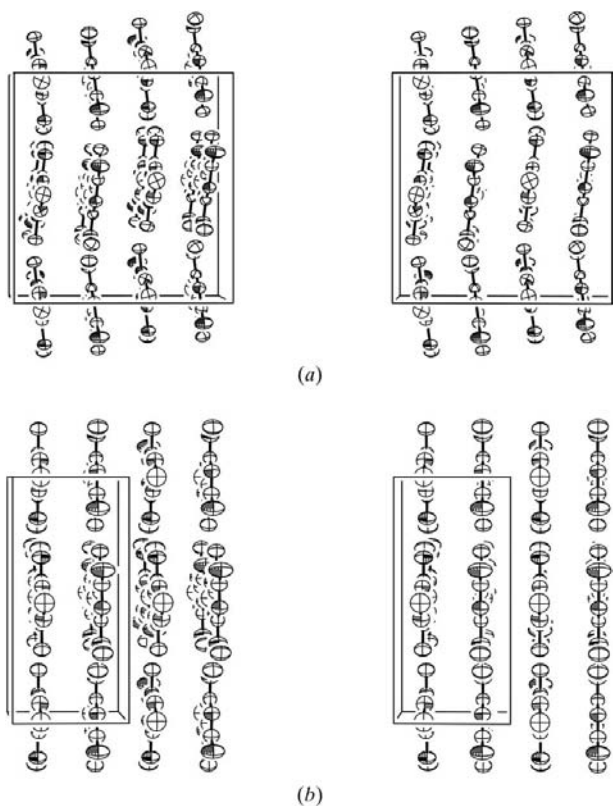


**Figure 3**  
Stereoscopic side view of (a) the low-temperature phase down the *c* axis and (b) the high-temperature phase down the *a* axis.

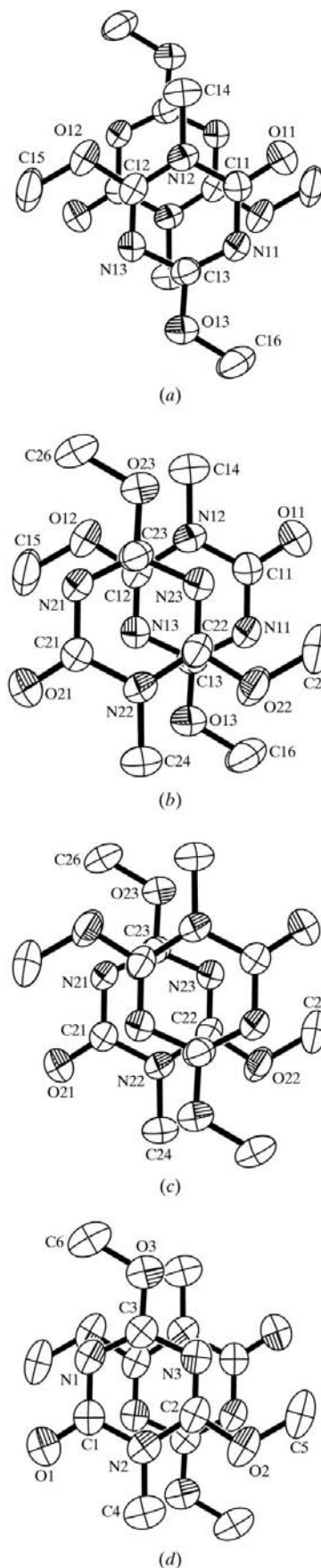


**Figure 4**  
Overlap diagrams of pairs in the LTP and HTP.

is quite a common feature of this group of compounds. For example, 1,4-dichlorobenzene (Wheeler & Colson, 1976; Maiga *et al.*, 1984) exists in three modifications: in the two monoclinic modifications the molecules adopt the herringbone packing motifs and in the triclinic modification the molecules adopt the stack packing motifs. The structures are closely related and therefore a reversible phase transformation may occur (Mnyukh, 1963). During our study of the solid-state methyl rearrangement in cyanurates and thiocyanurates (Kaftory & Handelsman-Benory, 1994; Handelsman-Benory, Botoshansky *et al.*, 2000; Greenberg *et al.*, 2001) we have found that both 2,4,6-trimethoxy-1,3,5-triazine (3) (Belaj & Nachbaur, 1987; Krygowski *et al.*, 1997; Handelsman-Benory *et al.*, 2000) and 4,6-dimethoxy-3-methyl-1,3,5-triazine-2(3*H*)-thione (4) (Greenberg *et al.*, 2001) crystallize in two different modifications. Both compounds crystallize either in the orthorhombic space group *Pnma*, adopting the stack packing motifs with the molecules occupying the mirror site symmetry, or in the monoclinic space group *P2<sub>1</sub>/c*. Upon heating the orthorhombic polymorph of (3) undergoes a phase transformation to the monoclinic *P2<sub>1</sub>/c* space group, adopting the herringbone-packing mode, while (4) undergoes a phase transformation

from the monoclinic space group *P2<sub>1</sub>/c* to the orthorhombic space group *Pnma* (Greenberg *et al.*, 2001). In both cases the crystal structures were destroyed during the irreversible phase transformation. The DSC thermograph of (3) is given in Fig. 6 (Handelsman-Benory *et al.*, 2000). The first endothermic peak

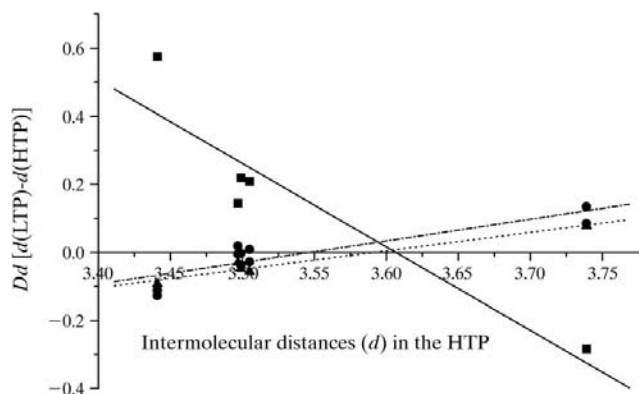


**Figure 5**  
The differences ( $\Delta d$ ) between the LTP and HTP intermolecular distances ( $d$ ) in each pair within a stack. Squares: *A·A*; circles: *A\*B*; triangles: *B·B*.

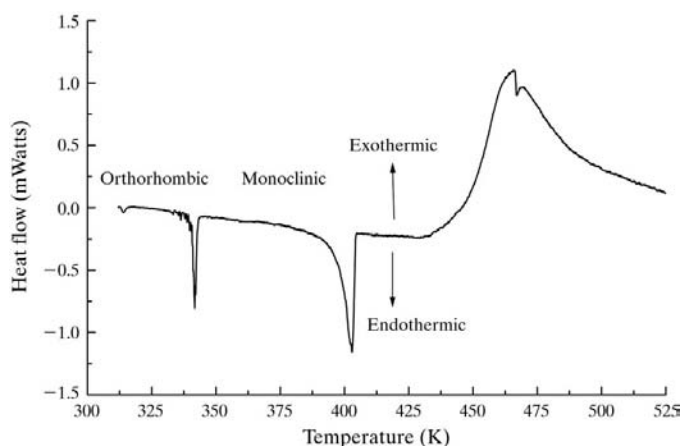


**Figure 6**  
DSC thermograph of (3) taken at a heating rate of  $1^\circ \text{min}^{-1}$ .

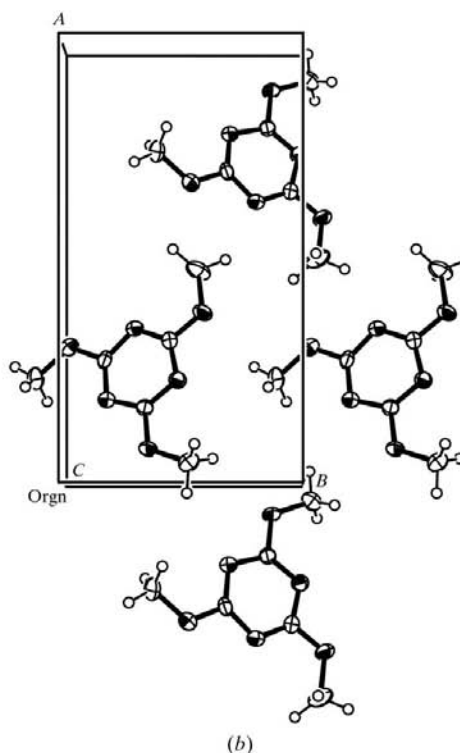
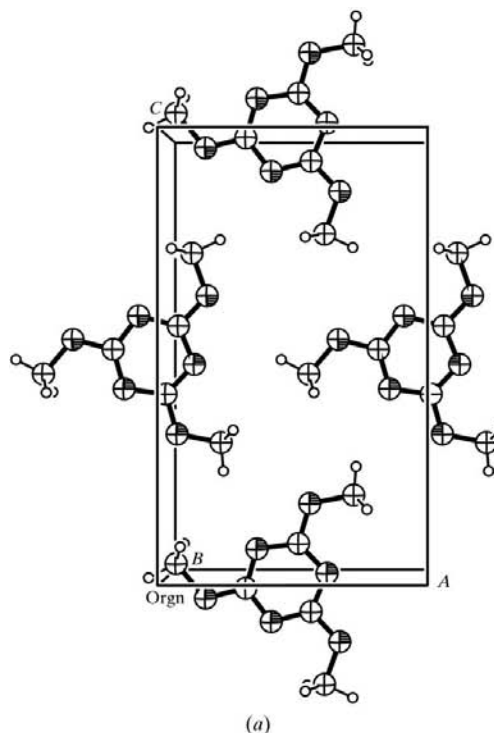


**Figure 7**  
(a) Structure of a layer of the orthorhombic phase of (3) and (b) a top view of a tilted layer of the monoclinic phase of (3).

**Table 4**

Comparison between the shortest intermolecular distances ( $\text{\AA}$ ) within a layer of the LTP and HTP of (1).

LTP	LTP	HTP	HTP
O11—C24	i 3.080 (3)	3.011 (4)	v O1—C4
O11—C15	ii 3.479 (3)	3.479 (5)	vi O1—C5
O13—C26	iii 3.214 (3)	3.350 (5)	vii O3—C6
N11—C15	ii 3.565 (3)	3.606 (5)	vi N1—C5
N13—C26	iii 3.525 (3)	3.652 (5)	vi N3—C6
C14—O21	iv 2.986 (3)	3.014 (4)	viii O1—C4
O21—C25	ii 3.500 (3)	3.473 (5)	ix—x O1—C5
O23—C16	3.398 (3)	3.348 (5)	ix O3—C6
N21—C25	iii 3.564 (3)	3.606 (5)	ix—x N1—C5
N23—C16	3.587 (3)	3.663 (5)	ix N3—C6

Symmetry codes: (i)  $x, -1 + y, z$ ; (ii)  $x, y, 1 + z$ ; (iii)  $x, y, -1 + z$ ; (iv)  $x, -1 + y, -1 + z$ ; (v)  $\frac{1}{2} + x, \frac{1}{2} - y, -\frac{1}{2} - z$ ; (vi)  $1 + x, y, z$ ; (vii)  $-\frac{1}{2} + x, y, \frac{1}{2} - z$ ; (viii)  $-\frac{1}{2} + x, \frac{1}{2} - y, -\frac{1}{2} - z$ ; (ix)  $\frac{1}{2} + x, y, \frac{1}{2} - z$ ; (x)  $\frac{3}{2} + x, y, \frac{1}{2} - z$ .

at 340 K with a measured enthalpy of  $3.9 \text{ kJ mol}^{-1}$  (the estimated  $\Delta S$  at this temperature is  $11.5 \text{ J mol}^{-1} \text{ K}^{-1}$ ) is assigned to the phase transformation. The second endothermic peak (at 389 K) is attributed to melting and the last exothermic peak (at 435 K) is assigned to the methyl rearrangement. The structure of a layer of (3) in the orthorhombic phase is shown in Fig. 7 (left), together with the structure of a layer of (3) in the monoclinic phase (Fig. 7, right). Side views of the packing in the unit cells of the two compounds are shown in Fig. 8.

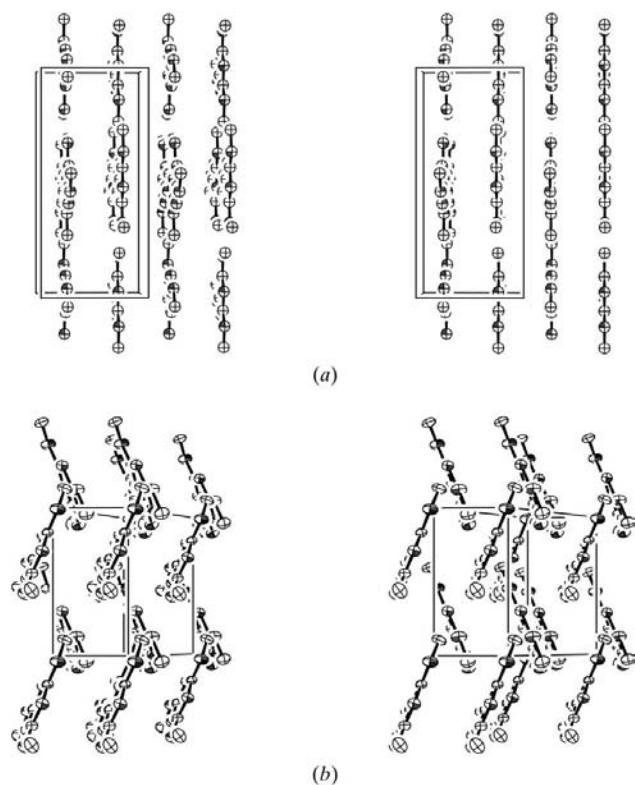


**Figure 8**

Stereo side view of (a) the orthorhombic phase of (3) down the  $a$  axis and (b) the monoclinic phase of (3) down the  $b$  axis.

**Table 5**

Comparison between intermolecular distances ( $d$  in  $\text{\AA}$ ) within a stack in the low- and in the high-temperature phases.

	$d(\text{HTP})$	$d(A \cdot A)$	$d(A \cdot B)$	$d(B \cdot B)$
N1—C2	3.505	3.714	3.477; 3.514	3.448
N2—C3	3.497	3.641	3.492; 3.516	3.467
N3—C1	3.499	3.718	3.496; 3.462	3.451
C1—C2	3.739	3.455	3.824; 3.873	3.817
C2—C3	3.441	4.016	3.314; 3.329	3.348

**Table 6**

Translation ( $\text{\AA}$ ), libration amplitudes ( $^\circ$ ) and weighted  $R$  for all  $U$ 's of molecules  $A$  and  $B$  in the low- and high-temperature phases at 320 and 359 K.

Molecule	$T_1$	$T_2$	$T_3$	$L_1$	$L_2$	$L_3$	Weighted $R$
LTP ( $A$ )	0.1988	0.1925	0.1763	5.30	3.84	3.34	0.076
LTP ( $B$ )	0.2033	0.1831	0.1694	5.68	3.57	3.30	0.092
HTP (320 K)	0.2509	0.2478	0.2182	6.60	4.05	3.54	0.076
HTP (359 K)	0.2561	0.2544	0.2109	7.06	4.40	4.16	0.074

The differences between the two forms are so large that the crystal structure of the orthorhombic form is destroyed during the phase transformation and is irreversible. Compound (1), on the other hand, undergoes a reversible single-crystal to single-crystal phase transformation. The phase transformation from monoclinic space group  $P2_1/n$  to the orthorhombic space group  $Pnma$  is followed by a variation of the unit-cell dimensions. Two of the unit-cell edges,  $a$  and  $c$  of the monoclinic LTP, vary continuously. However, the  $b$  axis of the HTP unit cell becomes half of the  $a$  axis of the LTP unit cell and the  $\beta$  angle changes to  $90.0^\circ$ . At the transition point, the last two parameters vary discontinuously, as expected for a first-order phase transformation. Nevertheless, the volume changes continuously (see Fig. 9).

The two phases are structurally only slightly different (see Figs. 2 and 3). The packing of the high-temperature modification seems to be an intermediate between the two pure modes of packing, stacking and herringbone. A statistical survey of the crystal structures of more than 100 compounds (Gould *et al.*, 1985) containing leucine, isoleucine, valine and phenylalanine residues shows that adjacent phenyl rings do not prefer an orientation with interplanar angles in the range  $5\text{--}30^\circ$ . This is due to the loss of stability gained when the molecules are in the stacking mode, without compensation stabilization that is reached in the herringbone packing where the interplanar angle is in the range  $40\text{--}90^\circ$  (Desiraju, 1989). The interplanar angle in the low-temperature modification of (1) is only  $15.77(3)^\circ$ . The small interplanar angle and the close resemblance of two of the three overlapping pairs prove that only a small amount of atomic movement is needed to convert the LTP structure into the HTP structure and that these conditions facilitate the phase transformation without destruction of the crystal lattice.

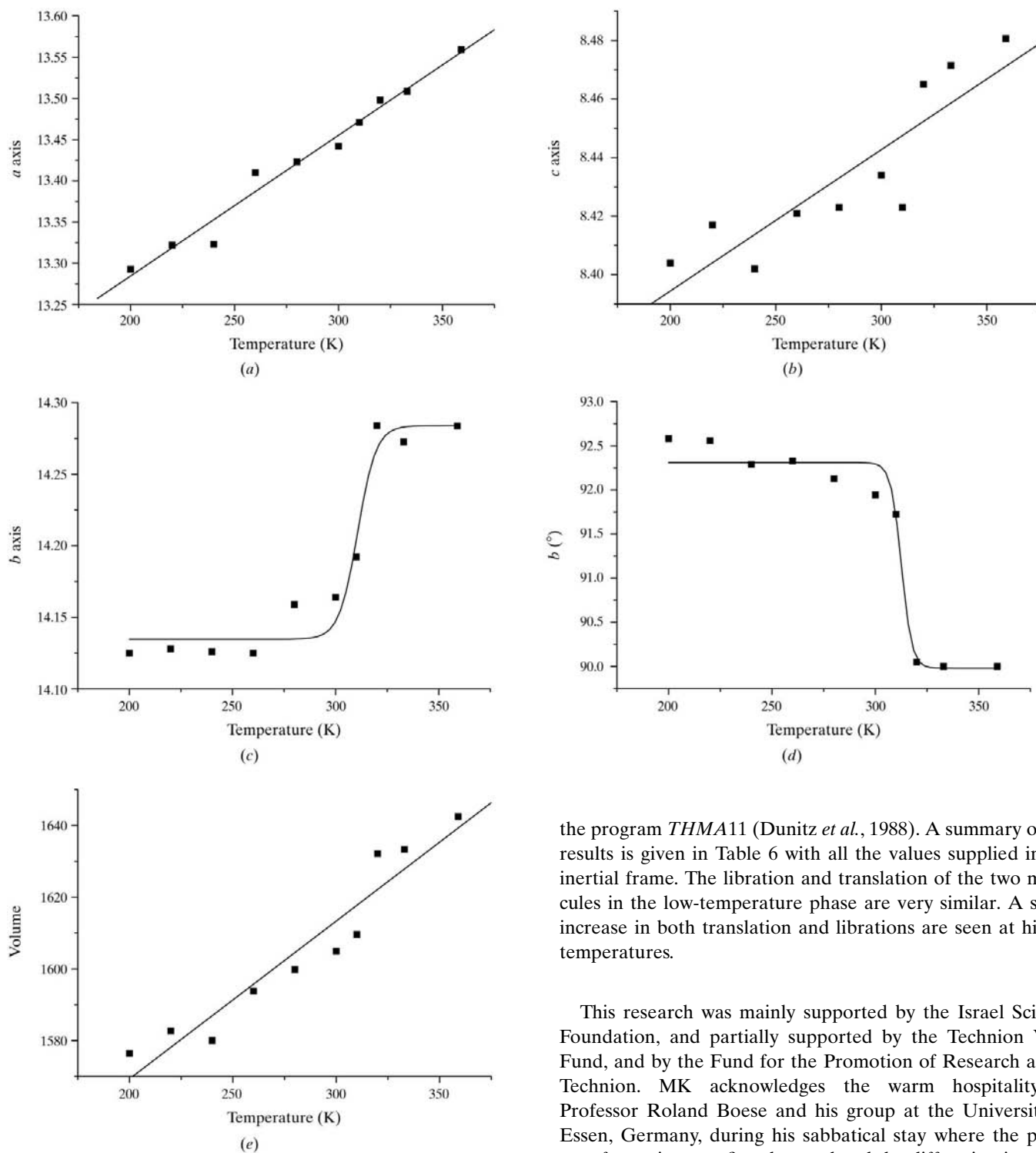


**Figure 9**  
Variation of the unit-cell dimensions of LTP and HTP as a function of temperature. The *a*, *b* and *c* axes of the LTP unit cell should be compared with *2b*, *c* and *a* axes of the HTP unit cell.

### 3.4. Thermal motion analysis

The thermal motion of the two molecules in the low-temperature phase and the single molecule of the high-temperature phase at 320 and 359 K has been analyzed with

the program *THMA11* (Dunitz *et al.*, 1988). A summary of the results is given in Table 6 with all the values supplied in the inertial frame. The libration and translation of the two molecules in the low-temperature phase are very similar. A slight increase in both translation and librations are seen at higher temperatures.

This research was mainly supported by the Israel Science Foundation, and partially supported by the Technion VPR Fund, and by the Fund for the Promotion of Research at the Technion. MK acknowledges the warm hospitality of Professor Roland Boese and his group at the University of Essen, Germany, during his sabbatical stay where the phase transformation was first detected and the diffraction intensity data was collected for the first time with a special experimental setup.

### References

- Belaj, F. & Nachbaur, E. (1987). *Monatsh. Chem.* **118**, 1077–1085.
- Desiraju, G. R. (1989). *Crystal Engineering*, Version 95. Amsterdam: Elsevier Science Publishers.
- Dunitz, J. D. & Bernstein, J. (1995). *Acc. Chem. Res.* **28**, 193–200.



- Dunitz, J. D., Maverick, E. F. & Trueblood, K. N. (1988). *Angew Chem. Int. Ed. Engl.* **27**, 880–895.
- Farrugia, L. J. (1997). *J. Appl. Cryst.* **30**, 565.
- Gafner, G. (1960). *Acta Cryst.* **13**, 706–716.
- Gafner, G. (1964). *Acta Cryst.* **17**, 982–985.
- Gould, R. O., Gray, A. M., Taylor, P. & Walkinshaw, M. D. (1985). *J. Am. Chem. Soc.* **107**, 5921–5927.
- Greenberg, M., Shteiman, V. & Kaftory, M. (2001). *Acta Cryst.* **B57**, 428–434.
- Handelsman-Benory, E., Botoshansky, M., Greenberg, M., Shteiman, V. & Kaftory, M. (2000). *Tetrahedron*, **56**, 6887–6897.
- Handelsman-Benory, E., Botoshansky, M. & Kaftory, M. (1995). *Acta Cryst.* **C51**, 2421–2424.
- Herbstein, F. H. (2000). *Advances in Structural Analysis*, edited by R. Kuel & J. Hasek. Praha: Czech and Slovak Crystallographic Association.
- Kaftory, M. & Handelsman-Benory, E. (1994). *Mol. Cryst. Liq. Cryst.* **240**, 241–249.
- Kitaigorodskii, A. I. (1970). *Adv. Struct. Res. Diffr. Methods*, **3**, 173.
- Krygowski, T. M., Howard, S. T., Martynowski, D. & Glowka, M. L. (1997). *J. Phys. Org. Chem.* **10**, 125–127.
- Maiga, A., Nguyen-Ba-Chanh, Haget, Y. & Cuevas-Diarte, M. A. (1984). *J. Appl. Cryst.* **17**, 210–211.
- McCrone, W. C. (1965). *Physics and Chemistry of the Organic Solid State*, edited by D. Fox, M. M. Labes & A. Weissberger, Vol. II, pp. 726–767. Interscience: New York.
- Mnyukh, Yu. V. (1963). *J. Phys. Chem. Solids*, **24**, 631–640.
- Mnyukh, Yu. V. (1977). *J. Cryst. Growth*, **38**, 284–291.
- Mnyukh, Yu. V. (1979). *Mol. Cryst. Liq. Cryst.* **52**, 467–503.
- Otwinowski, Z. & Minor, W. (1997). *Methods Enzymol.* **276**, 307–326.
- Nonius (1998). *Collect. Nonius BV*, Delft, The Netherlands.
- Paolini, L. & Tosato, M. L. (1968). *Ricerca Sci.* **38**, 552–553.
- Sheldrick, G. M. (1997a). *SHELXS97*. University of Göttingen, Germany.
- Sheldrick, G. M. (1997b). *SHELXL97*. University of Göttingen, Germany.
- Siemens (1995). *SMART and SAINT*. Siemens Analytical X-ray Instruments Inc., Madison, Wisconsin, USA.
- Tosato, M. L. (1979). *J. Chem. Soc. Perkin Trans. II*, pp. 1371–1375.
- Tosato, M. L. (1982). *J. Chem. Soc. Perkin Trans. II*, pp. 1321–1326.
- Wheeler, G. & Colson, S. D. (1976). *J. Chem. Phys.* **65**, 1227–1235.
- Zamir, S., Bernstein, J. & Greenwood, D. J. (1994). *Mol. Cryst. Liq. Cryst.* **242**, 193–200.